Vapor-Phase Spectra and the Pressure-Temperature Dependence of Long-Chain Carboxylic Acids Studied by a CO Laser and the Photoacoustic Heat-Pipe Detector

HENK JALINK, DANE BICANIC,* MLADEN FRANKO, and ZOLTÁN BOZÓKI

DLO Centre for Plant Breeding and Reproduction Research, CPRO-DLO, P.O. Box 16, 6700 AA Wageningen, The Netherlands (H.J.); Laser Photoacoustic Laboratory, Department of Agricultural Engineering and Physics, Agricultural University, Bomenweg 4, 6703 HD Wageningen, The Netherlands (D.B.); Department of Environmental Chemistry, Jozef Stefan Institute, Jamova 39, 61000 Ljubljana, Slovenia (M.F.); and Department of Quantum Electronics, JATE, University of Szeged, Dom Ter 9, H-6720 Szeged, Hungary (Z.B.)

A resonant photoacoustic heat-pipe (PAHP) cell was constructed and used for spectral studies of four long-chain saturated fatty acids (C10:0 to C16:0) at CO laser wavelengths and temperatures above that of the ambient. Vapor-phase absorption spectra were recorded at temperatures of 383 K for capric acid $C_{10}H_{20}O_2$, 400 K for lauric acid $C_{12}H_{24}O_2$, 438 K for myristic acid $C_{14}H_{28}O_2$, and 445.5 K for palmitic acid $C_{16}H_{32}O_2$, respectively. In addition, the temperature dependence (298 to 393 K) of vapor pressure was determined for C10:0; measurable PA signals were obtained at a temperature only a few degrees above the melting point for this acid. The data observed for C10:0 could be linearly fitted from as low as 323 K, indicating the validity of the Clausius-Clapeyron equation for temperatures lower than the 398 K < T < 541.4 K range anticipated so far.

Index Headings: **Vapor pressure; Saturated fatty acids; Infrared spectrum; CO laser; Clausius-Clapeyron equation; High-temperature photoacoustic cell; Heat pipe.**

INTRODUCTION

Liquid's tendency to vaporize increases with temperature and decreases with intensity of intermolecular forces. As a very good approximation, the vapor pressure of a given liquid depends solely on its temperature. The relationship between vapor pressure and temperature is nonlinear; it is, however, possible to convert the latter into a linear one by introducing new function of variables. The logarithm of vapor pressure (log p) plotted against the reciprocal of Kelvin temperature ($1/T$) yields a straight line $\log p = -A(1/T) + B$, known as the Clausius–Clapeyron equation. Numerical values of sample-specific A and B values are tabulated in various handbooks.[1] The most commonly used approaches to determine the vapor pressure/temperature curve are isoteniscopy, the gas saturation technique, and spectroscopy (although tedious).[2]

In (laser) photoacoustic (PA) spectroscopy, which has recently emerged as a highly sensitive method for studies of gases, the strength of the acoustic signal generated in the PA cell was found to be directly proportional to incident power, the magnitude of the temperature-dependent absorption cross section σ, and to the partial vapor pressure p of the measured species.[3–5] Real-time trace level concentration measurements were performed for a majority of atmospheric pollutants with the CO_2-laser-based PA method.[6]

Long fatty acids (number of C atoms in a chain exceeding 10) are representatives of low-volatility samples. As an example, capric acid C10:0 is solid at 293 K and has a vapor pressure of 0.8 mTorr.[7] One of the characteristic features in vapor-phase spectra of fatty acids in the infrared (IR), is the C=O bond centered near 1780 cm^{-1}; the latter vibration can readily be excited by the CO laser. The product $p\sigma$ for fatty acids is small in the IR, and hence vapor-phase spectra of fatty acids are obtained at temperatures significantly above that of the ambient. However, the usability of the traditional PA cell is limited by the maximum temperature to which the microphone and cell's optical components can be exposed. In addition, both windows and microphone are prone to contamination, in particular, when in contact with aggressive specimens such as, for example, fatty acids.

An elegant approach in circumventing problems of this kind is to incorporate the concept of the heat pipe (HP) into classical photoacoustic detection. A conventional heat pipe is normally used to promote heat transfer by thermal conduction.[8] Characteristic for a heat pipe is the confinement of the working fluid within well-defined hot and cold zones, and its wide (working fluid-dependent) range of operating temperatures. By interconnection of their hot zones, two such HPs are readily combined into a single photoacoustic heat pipe (PAHP), forming a cold zone at each end. The first PAHP (Fig. 1a) was a closed resonator;[9] it comprised a metal tube (heated externally) by means of a resistive coil **H** with windows **W** mounted either perpendicularly or under Brewster angle to the tube's longitudinal axis. The cell with a metal mesh **MM** (extending along the tube's horizontal axis from one water-cooling jacket **C** to another) was operated at a frequency corresponding to the second acoustic longitudinal resonance having maxima of pressures at each window and at the central portion (evaporator) of the tube (Fig. 1c). In order to avoid exposure to high temperatures, the microphone **M** was mounted as close as possible to a window **W** of the PAHP cell. The temperature distribution in the cell resembles that shown in Fig. 1b. Locating pressure maxima at cell windows represents a drawback of the closed-resonator PAHP design. This limitation is due to the fact that some fraction of the incoming radiation will always be absorbed by the cell windows, generating acoustic signal at actual modulation frequency; these unwanted signals couple to the cell and affect its ultimate sensitivity.

Consequently, an enhancement of sensitivity is antic-

Received 24 October 1994; accepted 23 March 1995.

* Author to whom correspondence should be sent.

0003-7028/95/4907-0994$2.00/0

ipated for a cell design capable of suppressing the contribution of window absorption to the PA signal. This paper is concerned with a novel photoacoustic heat-pipe detector. Unlike all previous designs, the PAHP device (Fig. 2a) developed and used in the study described here is an open resonator featuring identical acoustic baffles at each end of the tube. Spatial distribution of temperature and pressure for such an open-resonator PAHP is shown in Fig. 2b and 2c. In the original PAHP design (Fig. 1a), the windows were glued directly to the resonator—quite impractical if the latter is to be replaced. This shortcoming was overcome in a new PAHP design allowing easy and rapid interchangment of both sample and mesh, as well as a quick replacement of the entire resonator tube (disposable).

In this paper, the feasibility of an open-resonator PAHP cell for recording IR vapor-phase spectra and the pressure/temperature dependence of fatty acids is demonstrated. Contrary to the "indirect" approach (often used in practice), where pressure/temperature curves for fatty acids are recorded at temperatures substantially above their melting points before results are extrapolated to lower temperatures, in this work the dependence was determined directly. Vapor pressure/temperature dependence was measured for C10:0 in a 323 to 541.5 K range with the use of a CO laser as the excitation source; results obtained were compared to those predicted by the Clausius–Clapeyron equation. In addition, vapor-phase spectra of various even (C10:0 to C16:0) saturated fatty acids were obtained at several temperatures. The methodology and instrumentation proposed here apply to other nonvolatile liquids and solids as well.

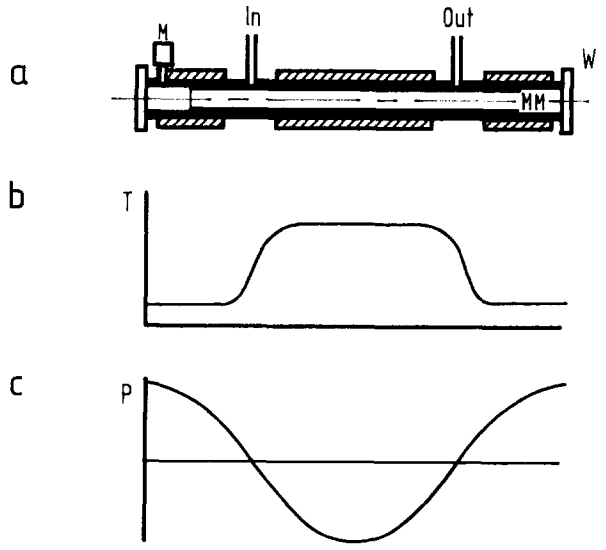

FIG. 1. The photoacoustic (closed-resonator) heat pipe, PAHP, (**a**) containing metal mesh **MM** and the miniature microphone **M** positioned near the cooling jacket and entrance window **W**. Heating of the tube is achieved by a direct current flowing through resistive coil **H**. The temperature (**b**) and the amplitude of pressure wave (**c**) are plotted against position (in the axial direction) within the PAHP cell.

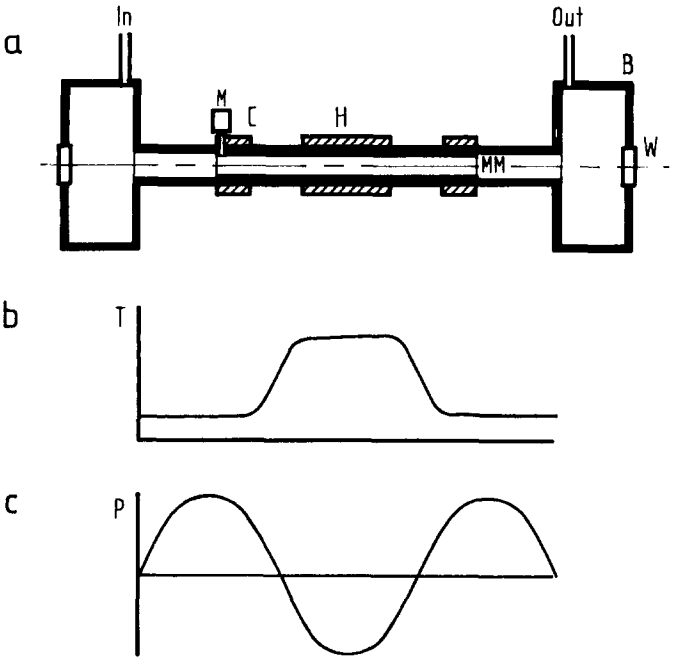

FIG. 2. Open-resonator photoacoustic heat pipe (**a**) showing baffles **B** (for supression of signals due to absorption of radiation in window **W**), resistive coil **H**, metal mesh **MM**, and a microphone **M** (integrated in a water cooling jacket **C**). The microphone is removed from the window **W** and mounted at one of the pressure maxima. Spatial distribution of temperature (**b**) and pressure (**c**) for such open-structure PAHP is also shown.

EXPERIMENTAL

The exploded view of the new, open PAHP resonator is shown in Fig. 3. The heart of the cell is a 210-mm-long resonator tube (inner diameter, 9 mm; outer diameter, 11 mm) made of quartz glass (**7**) and provided with a resistive heater (**5**) (constantan wire, 0.5 mm diameter) wrapped (heated length, 40 mm) around the tube's central section (glass sleeve provided electrical insulation between adjacent windings). The copper-constantan thermocouple is inserted between the heater and tube's outer wall to monitor the temperature at the evaporator. The tube is equipped with a water-cooled jacket (**4**) at each end. In an arrangement to promote efficient heat transfer, running water is in direct contact with the outer wall of the quartz tube (two O-rings in each jacket were used to provide the seal). The microphone (**3**), a miniature electret M32 manufactured by Microtel BV Amsterdam, is fully integrated into a jacket and acoustically coupled to the resonator via a circular hole (2.5-mm diameter) drilled in the tube's wall. The position of this opening (35 mm from the left end of a quartz tube in Fig. 2a) coincides with that of the first pressure maximum of the third longitudinal resonance. A 25-mm × 130-mm piece of a stainless steel (250 openings per inch) metal mesh (**6**), manufactured by Wire Weaving Company Dinxperlo, The Netherlands, was folded to form a single layer and inserted into the resonator; it extended (130 mm) in the axial direction from one water-cooled jacket to another. In an arrangement to minimize window signal, the cell is provided with two identical acoustic baffles (**2**) (length, 35 mm; width, 40 mm; and height, 40 mm at both sides of the resonator) closed from above by aluminum flange and rubber O-ring seal. The same flange also carries inlet and outlet ports for admission and removal of a major gaseous component in the mixture (here nitrogen of very high purity). The baffles function as acoustic chokes and

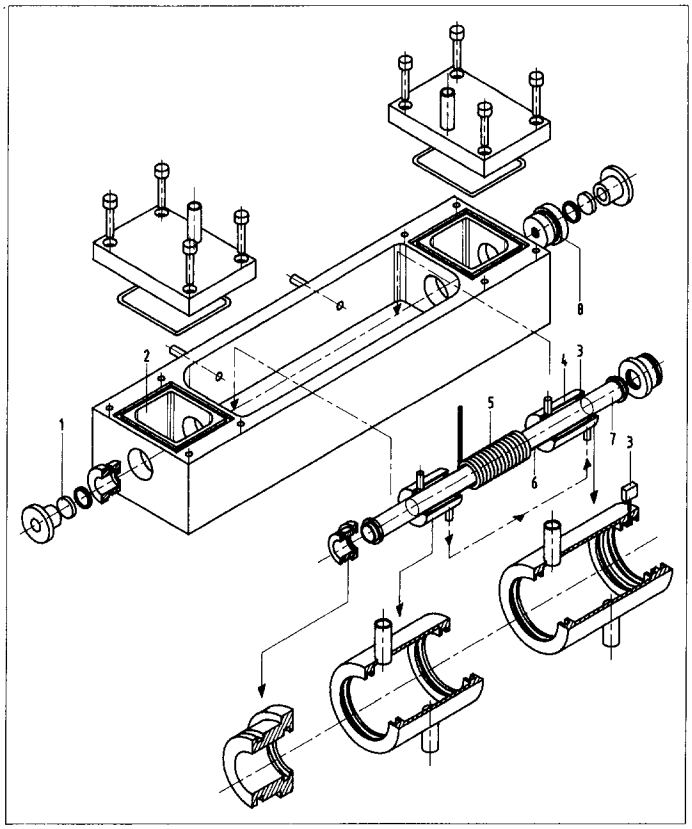

FIG. 3. Exploded view of open-resonator PAHP consisting of windows (1); acoustic baffles (2); O-ring seals with miniature microphone (3) (see detail) fully integrated into cooling jacket (4); resistive heater (5) with thermocouple and power supply, metal mesh (6); disposable quartz tube (7); and protective caps (8).

prohibit (by the virtue of their precisely defined length) efficient coupling of the window signal into the resonating structure of the cell. The physical length of each baffle is equal to a quarter of the resonant acoustic wavelength λ. Two flat CaF_2 disks (12.7-mm diameter and 3-mm thick) are mounted in holders perpendicularly to the resonator and function as cell windows (**1**). The resonator tube itself was accommodated in a housing (length, 300 mm; width, 80 mm; height, 50 mm) milled from a solid piece of anodized aluminum. Bringing a tube into position was achieved by means of protective caps (**8**), each provided with two O-rings; the principal function of the outer (and inner) O-rings is to maintain the seal between a baffle (the resonator) and ambient air.

With one of the windows (**1**) removed, loading of the cell was performed at 293 K by depositing the sample (typically some 50 mg of fatty acid) on a metal wick (**6**) while ensuring good thermal contact (needed for optimal capillary working) between the wick and tube's (**7**) inner walls. The cell was first evacuated (10^{-2} mbar) before dry nitrogen was added to reach a total pressure of 1000 mbar. As the temperature at the evaporator increases gradually, the sample begins to melt and is uniformly distributed along the wick. At a certain temperature, vaporization causes an increase of pressure that leads to a transport of vapor towards water-cooled regions (condensers). The mesh's capillary forces and a positive pressure difference in the liquid (between the condenser and evaporator) force the liquid to return to the evaporator after condensation of the vapor has taken place. Eventually, a dynamic equilibrium is reached, implying the simultaneous occurrence of two opposing processes in a closed system (in such a way as to offset one another). Since, at a given temperature, the flux of evaporating molecules equals that undergoing condensation, the number of molecules in the vapor phase becomes constant and no additional vapor is formed. Sharply defined interfaces (between the evaporator and the two condensers), formed at both sides of the vapor column, separate the mixture (vapor/nitrogen) from the buffering gas. Because of this arrangement, direct contact between the fatty acid and the microphone (and windows too) is prevented; these latter remain therefore at a room temperature. The perpetual process of vaporization and condensation is a reason for the radiation to be absorbed only within the heated zone trapped between two interfaces.

In a procedure to replace the wick, the resonator tube (**7**) (with both cooling jackets and heating coil), is demounted by first pushing (inwards) protective caps (**8**) before removing the tube out of the housing. After the dismantling of the protective caps and jackets, the tube is gently brushed and rinsed (ethanol and washing detergent) before distilled water spooling and hot gun drying. Reassembling of the PAHP cell takes place in the reverse order.

Operating the PAHP cell in resonant mode offers two important advantages above the nonresonant regime. In the first place, resonant operation suppresses parasitic window signals by the resonator's quality factor Q (defined as the ratio of the center frequency and the full frequency bandwith at half peak height). Furthermore, higher modulation frequencies can be used since, at resonance, the loss of signal (due to $1/f$ dependence) is partially compensated by the Q factor. In principle, any mode can be excited in an open-resonator PAHP when vapor distribution in axial direction is not homogeneous. However, only odd modes are excited for symmetric distributions.

The acoustic wavelength λ associated with the longitudinal resonant mode of a standing wave generated in a tube of length L satisfies $L = n\lambda/2$, with n being an integer ($n = 1, 2, 3 \ldots$). Three lowest longitudinal modes in a cell of length L are displayed in Fig. 4. The length L (210 mm) of the quartz resonator (**7**) used in this study satisfies $L = 3\lambda/2$. As shown in Fig. 4, this implies the occurrence of three ($n = 3$) equal-pressure maxima, two of them located at water-cooled regions and a third one in a "hot zone" (inaccessible for the microphone). The amplitudes of PA signals generated at these three maxima are comparable, but phases at cold and hot regions differ by 180°.

The PAHP cell was irradiated with a homemade cw and grating-tunable, cryogenic CO laser operated at 233 K. The laser radiation (the identity of emitting laser line was determined by a Laser Optical Engineering spectrum analyzer) was mechanically chopped (PTI Model OC4000) before being focused by a CaF_2 lens ($f = 200$ mm) to form a spot in the PAHP cell at the center of the heated zone. The microphone signal and chopper reference were fed into an Ithaco 3961 two-phase lock-in amplifier for synchronous detection at the modulation frequency. The current through the wires of the resistive heater was con-

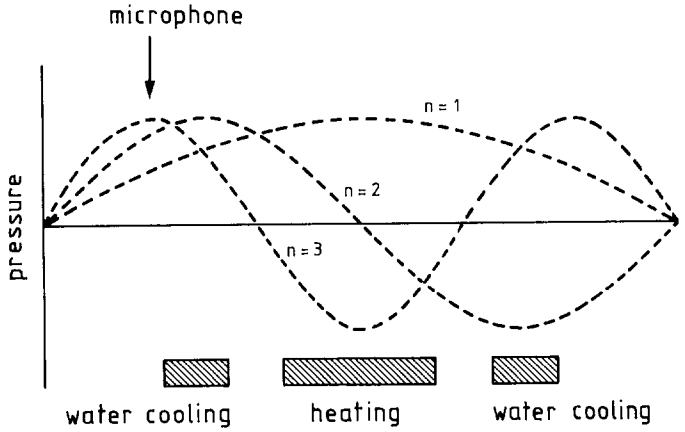

FIG. 4. Pressure distribution for three lowest longitudinal modes excited in an open resonator. Positions of microphone, water cooling jacket, and resistive heater are specified.

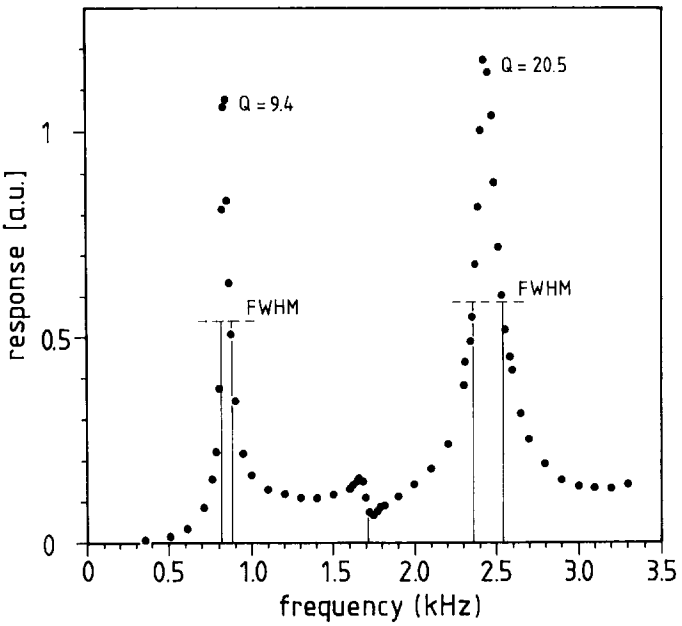

FIG. 5. The frequency characteristics of the PAHP cell shown in Fig. 3 showing positions of three lowest longitudinal resonances and their corresponding quality factors (FWHM is full width at points of half-maximum). This figure was recorded at 413.5 K and 1000 mbar with methylsterate as a sample and the 10R(22) transition of a CO_2 laser.

trolled by a Philips PE 1539 stabilized power supply, and the temperature of the cell's outer wall determined by reading off a thermocouple voltage on a Keithley 177 digital voltmeter. For the purpose of signal normalization, power emitted by the CO laser was measured by a homemade PVDF pyroelectric detector in combination with an EG&G 5101 lock-in amplifier. All fatty acids (purity larger than 90%) were kindly supplied by Unilever Research Laboratory, Vlaardingen, The Netherlands.

RESULTS AND DISCUSSION

The frequency (0 to 3.5 kHz) characteristics of the PAHP cell shown in Fig. 3 was determined in an independent experiment by irradiating a mixture of methylstearate and nitrogen with radiation of the CO_2 laser tuned to the 10R(22) transition. The results of the measurements (performed at 1000 mbar and 413.5 K) are displayed in Fig. 5. Two pronounced peaks (the corresponding Q factors are 9.4 and 20.5) centered at 870 Hz and 2450 Hz are observed; a smaller third peak appears near 1650 Hz. Substituting $L = n\lambda/2$ for longitudinal resonances into $c = f\lambda$ (c is the velocity of sound in a given medium under actual operating conditions), one has $f = nc/2L$. With $L = 0.21$ m and $c = 330$ m/s, it follows that $f = 786$ Hz for the first ($n = 1$) peak in Fig. 5; the same expression gives 1571 and 2357 Hz for higher ($n = 2$ and 3) harmonics of the fundamental longitudinal resonant frequency. The difference between the calculated (786-Hz) and experimentally found (880-Hz) resonant (for $n = 1$) frequency is probably due to the velocity being other than 330 m/s (taken in calculations above), the possibility that the position of the pressure node is not exactly at the resonator's end, and the realization that the Q factor itself is also temperature dependent.

Vapor-phase spectra of C10:0, C12:0, C14:0, C16:0, and C18:0 saturated fatty acids were determined next at 1000 mbar. The operating temperature varied from 383 K for C10:0 to 445.5 K for C16:0. Once the desired temperature was reached, it remained stable (within 0.05 of a degree) for longer time intervals. Fluctuations in the amplitude of the microphone signal (1%) are mainly due to temperature changes (logarithmic dependence of the sample's vapor pressure on the reciprocal of the temperature) at the evaporator. The measurements were performed close to a 2450-Hz resonance; precise tuning of modulation frequency into actual resonance was, however, performed for each temperature and for each fatty acid. Results showing normalized PA signals plotted vs. wavenumbers of CO laser transitions are displayed in Figs. 6A–6D. All spectra have a similar shape and exhibit the peak associated with the C=O functional group near 1780 cm^{-1}. Fitting the spectra by a Lorentzian profile gives peak positions at 1780.31 cm^{-1} (for C10:0), 1779.38 cm^{-1} (for C12:0), 1779.77 cm^{-1} (for C14:0), and 1778.81 cm^{-1} (for C16:0). The halfwidth of the peak at the points of half-maxima is 27.25 cm^{-1} (for C10:0), 27.47 cm^{-1} (for C12:0), 31.68 cm^{-1} (for C14:0), and 34.73 cm^{-1} (for C16:0). The shift of a strong C=O carbonyl band (in dimeric form at 1712 cm^{-1}) to higher wavenumbers is expected when going from a liquid into a gas phase.[10,11]

Finally, with the CO laser tuned to a frequency of the C=O vibration, PA signals from C10:0 were measured within the 305 to 410 K range. At a given temperature, the PAHP was operated in static (nonflowing) mode at a total pressure of 1000 mbar, and at a modulation frequency corresponding to the third ($n = 3$) longitudinal acoustic resonance near 2450 Hz. The CO laser power was kept constant throughout the measurement. The actual amplitude (in μV) of the microphone signal (fed to the lock-in amplifier) plotted against temperature in °C (upper horizontal axis) and as a function of the reciprocal of the absolute temperature (lower horizontal axis) is shown in Fig. 7. The validity of the Clausius–Clapeyron equation, $\log p = -0.2185A/T + B$ (with p in Torr and T in degree of Kelvin) for capric acid ($A = 19372.6$ and $B = 10.872662$), is restricted to a 125°C (398 K) to 268.4°C (541.4 K) temperature range.[1] Clearly, since a 398 K limit is only a few degrees below the highest temperature (410 K) used in our study, the proposed methodology and

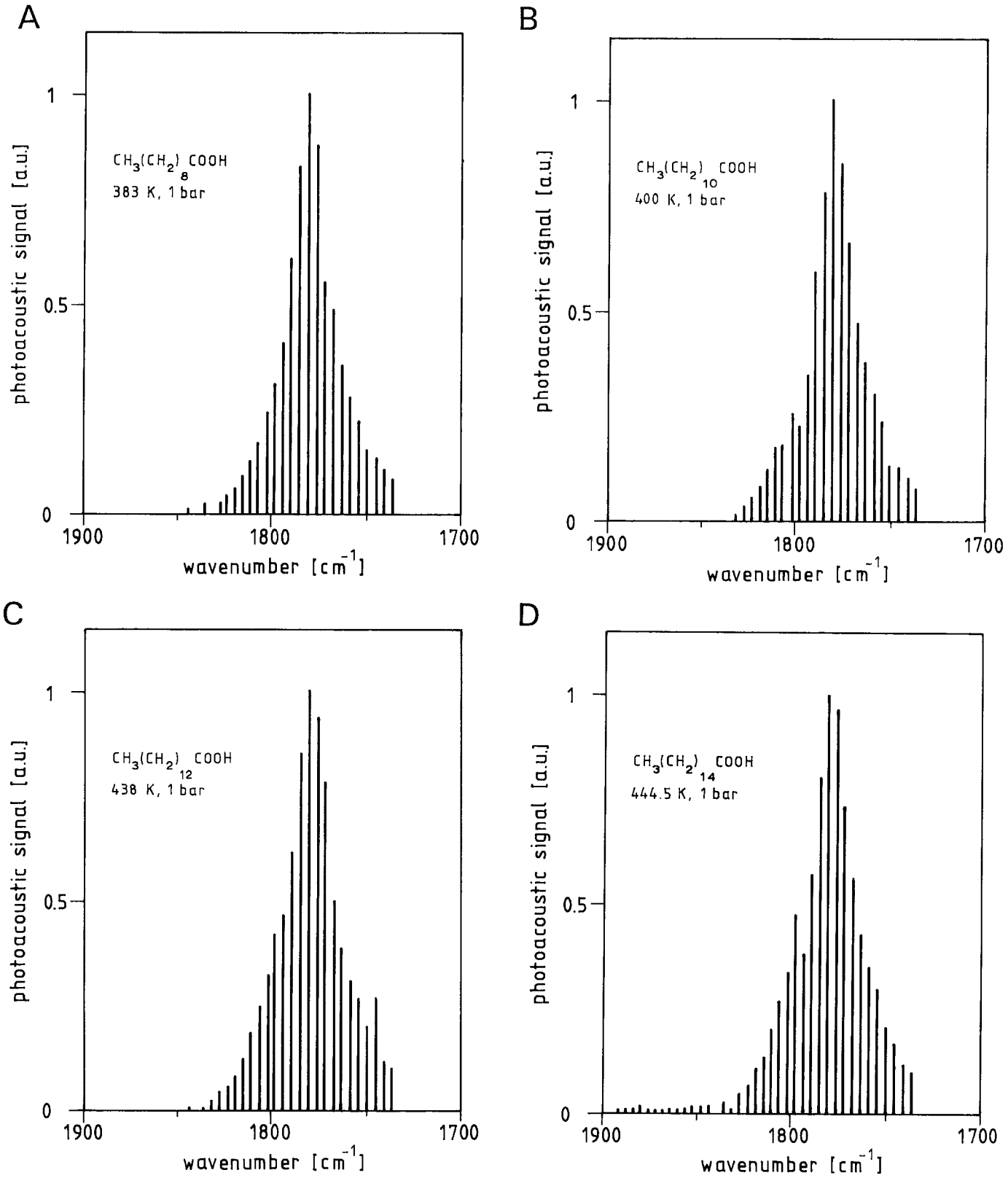

FIG. 6. The CO laser photoacoustic spectra of capric (**A**), lauric (**B**), myristic (**C**), and palmitic (**D**) saturated fatty acids in clean nitrogen recorded at 383, 400, 438, and 445.5 K, respectively, with the PAHP from Fig. 3. Total pressure in the PAHP was 1000 mbar; the cell was operated at a modulation frequency (approximately 2450 Hz) corresponding to that of the third ($n = 3$) longitudinal resonance.

instrumentation developed here offer the possibility of experimentally testing (for C10:0) the validity of the present Clausius–Clapeyron equation at temperatures significantly lower than previously anticipated.

Substituting numerical values for A and B into the above equation, one obtains a vapor pressure of 1.3 Torr for C10:0 at 120°C (393 K). The corresponding microphone signal was about 3 mV. Data points in Fig. 7 represent

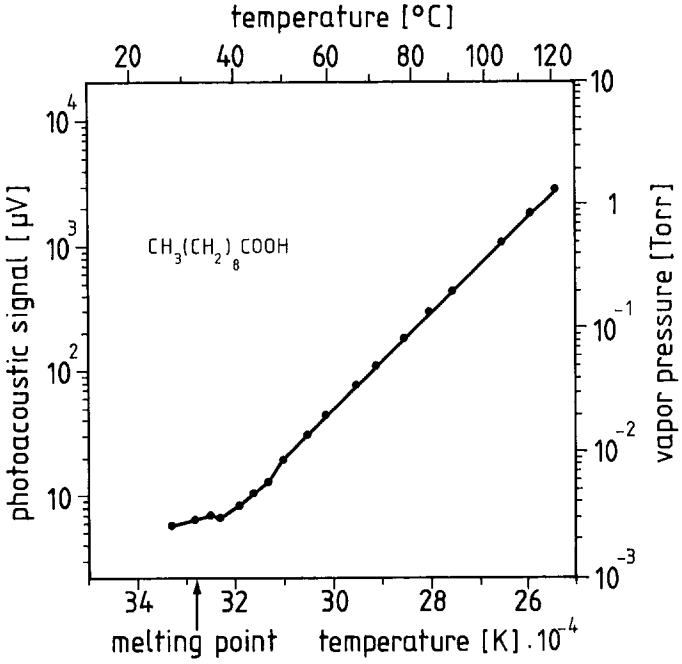

FIG. 7. Photoacoustic signals (vertical axis left) obtained with capric acid at different temperatures (the lower horizontal axis is the reciprocal of the absolute temperature, while the upper horizontal axis is the temperature in degrees of Celsius). The total pressure of a C10:0/N_2 mixture in the PAHP cell was 1000 mbar. Vapor pressures calculated at various temperatures by means of the Clausius–Clapeyron equation (with A and B constants for capric acid) are plotted along the vertical scale (at right). The melting point for capric acid is indicated by an arrow.

the magnitude of the PA signals measured at various temperatures. When the logarithm of the PA signal is plotted against $10^4/T$, a linear relationship is obtained within the 393 to 310.6 K ($10^4/T$ = 32.2) range. This result implies a direct proportionality between the PA signal and the vapor pressure. Most likely, at these temperatures (the dimers formed by fatty acids in the condensed phase are completely dissociated), monomers dominate the vapor-phase spectrum. The slope of the line is the same as that predicted by the Clausius–Clapeyron equation for temperatures from 398 to 541.4 K. At still lower temperatures, a deviation from a straight line is observed (Fig. 7). At 293 K, the PA signal was 5.6 μV; unexpected is a slight drop of signal strength close to the melting point of C10:0. Perhaps this observation is an indicator of the presence of a dimeric form that still exists in the gas phase at lower temperatures.

In conclusion, the usability of the resonant photoacoustic heat-pipe cell (with metal mesh) for recording IR vapor-phase spectra of long-chain fatty acids at temperatures above that of the ambient was demonstrated. Without the mesh, PA signals were typically three to four orders of magnitude lower and the reproducibility of measurements was very poor. This simple, low-cost device allowed determination of a vapor pressure/temperature curve for capric acid. The results present, to the best of the authors' knowledge, the first experimental evidence for the validity of the Clausius–Clapeyron equation (for C10:0) in a temperature range lower than anticipated so far. The methodology and apparatus are extendable to other spectral and temperature ranges and can be used with arbitrary nonvolatile liquid or solids provided that excitation of the sample can be achieved. In the future, the PAHP might also prove a convenient tool in determining (directly) the heat of vaporization of liquid samples; work on this effort is already in progress.

ACKNOWLEDGMENTS

The research described in this work was partially supported by the Unilever Research Laboratory, Vlaardingen, The Netherlands; the Dutch Organization for Scientific Research, NWO, The Hague; and the European Community (Science Twinning Program). The authors are grateful to departmental mechanical, glass, and electronic workshops for technical assistance, and to Mees Schimmel and Piet Versteeg for skilled illustration work.

1. *Handbook of Physics and Chemistry,* R. C. Weast, Ed. (Chemical Rubber Company, Cleveland, Ohio, 1971, 51st ed.
2. R. H. Petrucci, *General Chemistry: Principles and Applications* (Macmillan Publishing Co., Collier Macmillan Publishers, London, 1982), 3rd ed.
3. J. Davidsson, J. H. Gutow, and R. N. Zare, Jour. Phys. Chem. **94,** 4069 (1990).
4. *Photoacoustic and Photothermal Phenomena III,* D. Bicanic, Ed., Springer Series in Optical Sciences 69 (Springer Verlag, Heidelberg, 1992).
5. D. Bicanic, M. Chirtoc, C. van Asselt, E. Gerkema, H. Jalink, H. Sauren, T. Groot, P. Torfs, and K. Haupt, Acta Chim. Sloven. **40,** 175 (1993).
6. *Air Monitoring by Spectroscopic Techniques,* M. Sigrist, Ed. (John Wiley and Sons, New York, 1994).
7. M. L. Meara, *Physical Properties of Oils and Fats,* Scien. Tech. Surveys 110 (Food Research Association, Leatherhead, U.K. 1985).
8. D. Chisholm, *The Heat Pipe* (Mills and Boon, London, 1971).
9. H. Jalink and D. Bicanic, Appl. Phys. Lett. **55,** 1507 (1989).
10. R. A. Nyquist, *The Interpretation of Vapor Phase Infrared Spectra,* Vol. 1, *Group Frequency Data* (Heyden, London, 1984).
11. D. Welti, *Infrared Vapor Spectra* (Heyden and Son, London, in cooperation with Sadtler Research Laboratories, Philadelphia, 1970).